



2013

Background Paper prepared for the Global Assessment Report on
Disaster Risk Reduction 2013

Tsunami methodology and result overview

Norwegian Geotechnical Institute (NGI)



Geneva, Switzerland, 2013

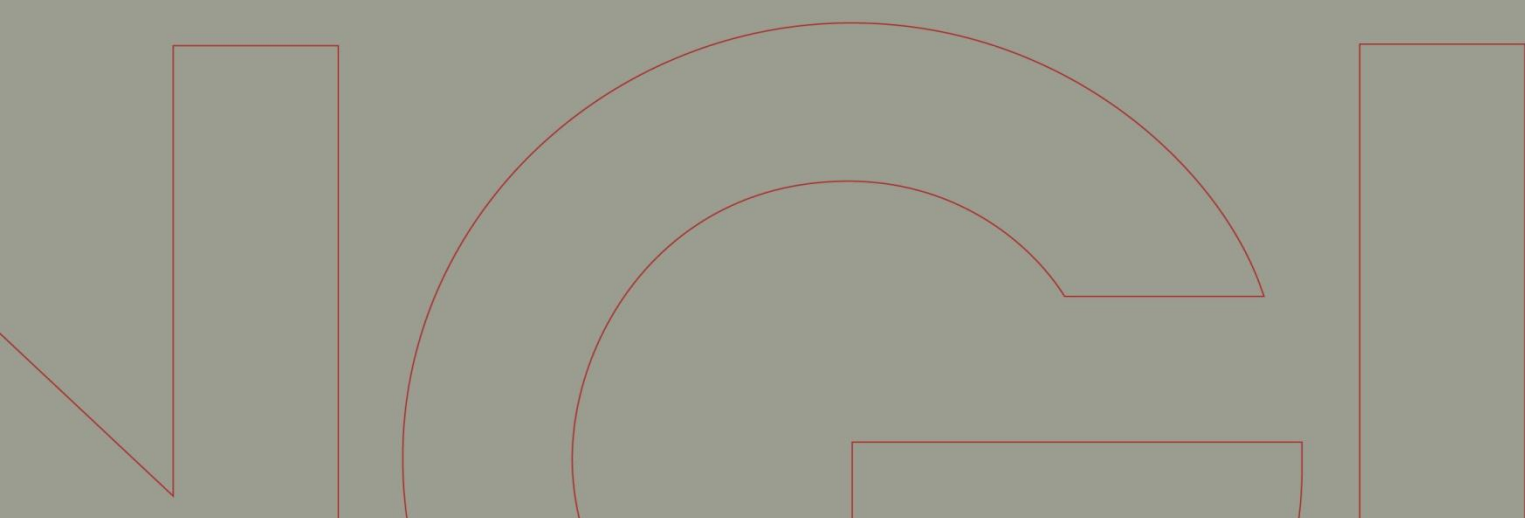


Rapport / Report

UNISDR Global Assessment Report 2013 - GAR13

Tsunami methodology and result
overview

20120052-02-R
21 March 2013
Revision 1



Ved elektronisk overføring kan ikke konfidensialiteten eller autentsiteten av dette dokumentet garanteres. Adressaten bør vurdere dette før bruk av dokumentet.

Dokumentet skal ikke benyttes i utdrag eller til andre formål enn det dokumentet omhandler. Dokumentet må ikke reproduseres eller leveres til tredjemann uten eiers samtykke. Dokumentet må ikke endres uten samtykke fra NGI.

Neither the confidentiality nor the integrity of this document can be guaranteed following electronic transmission. The addressee should consider this before using this document.

This document shall not be used in parts, or for other purposes than the document was prepared for. The document shall not be copied, in parts or in whole, or be given to a third party without the owner's consent. No changes to the document shall be made without consent from NGI.



Project

Project: UN-ISDAR Global Assessment Report 2013
– GAR 2013
Report No.: 20120052-02-R
Report title: Tsunami methodology and result overview
Date: 11 March 2013

Main office:
PO Box 3930 Ullevål Stadion
NO-0806 Oslo
Norway

Trondheim office:
PO Box 1230 Pirsenteret
NO-7462 Trondheim
Norway

T (+47) 22 02 30 00
F (+47) 22 23 04 48

BIC No. DNBANOKK
IBAN NO26 5096 0501 281
Company No.
958 254 318 MVA

ngi@ngi.no
www.ngi.no

Client

Client: The United Nations Office for Disaster Risk
Reduction – UNISDR
Client's contact person: Andrew Maskrey
Contract reference: Signed agreement dated 16 November 2012

For NGI

Project manager: Farrokh Nadim
Report prepared by: Finn Løvholt, Sylfest Glimsdal, Helge
Smebye (NGI), and Nick Horspool
(Geoscience Australia)
Reviewed by Carl B. Harbitz

Summary

The present paper gives a brief overview of the tsunami component of the Global Assessment Report 2013, involving a global hazard and exposure analysis with emphasis on population and critical facilities. Tsunamis are infrequent events with the power to cause massive loss of life, large economic losses, and cascading effects such as destruction of critical facilities. Infrequent, but large and highly destructive tsunami events generally pose greater risk than the cumulative effect of smaller and more frequent events. The tsunami hazard is therefore quantified with a return period of 500 years. Furthermore, the analysis is constrained to tsunamis induced by earthquakes. Two different methods are applied for establishing the hazard. For the Indian Ocean and the South West Pacific, a probabilistic method (PTHA) is applied. For all other areas, a scenario based method similar to the one applied for GAR 2009 is adopted. The damage metric used in the analysis is the maximum run-up, which is

BS EN ISO 9001
Certified by BSI
Reg. No. FS 32989

Summary (cont.)



Report No.: 20120052-02-R
Date: 2013-03-21
Revision: 1
Page: 2

determined using the method of amplification factors for both hazard methods. The analysis shows that populous Asian countries, most prominently Japan, but also China and Indonesia account for a large absolute number of people living in tsunami prone areas. This is due to the combination of large hazard and dense population. A similar hazard is found along the US and South American coastlines, but here the total exposure are smaller. In relative exposure, smaller countries like Macau and the Maldives are among the highest ranked countries. In these countries, a higher amount of the total population is exposed to tsunamis. The analysis of exposure of critical facilities includes nuclear reactors and airports. Japan has the largest number of nuclear power plants within the inundated area (7). In certain areas such as the eastern United States and the United Kingdom, landslide induced tsunamis may constitute an additional significant threat towards critical facilities, but these tsunami sources are not included in the current statistics, even though near shore critical facilities may in general be exposed to this additional threat. Compared to GAR 2009, the current update provides an almost complete global coverage. As a result, the population exposure in total is higher. Furthermore, industrialized countries dominate the critical facilities statistics.

Contents



Report No.: 20120052-02-R
Date: 2013-03-21
Revision: 1
Page: 3

1	Introduction	4
2	Methodology	5
2.1	Design of the earthquake scenarios	5
2.2	Wave propagation modelling	12
2.3	Employed Probabilistic Tsunami Hazard Assessment method	13
2.4	Run-up estimation and inundation mapping using amplification factors	15
2.5	Inundation mapping and exposure	18
3	Results	19
4	Limitations, sources of error and look ahead	28
4.1	Return periods	28
4.2	Non-seismic sources	28
4.3	Interpretation of hazard maps and population exposure	29
4.4	Risk assessment	29
5	References	30

Review and reference page

1 Introduction

The size of recent large scale tsunamis in Sumatra 2004 and Tohoku 2011 was to a large degree unexpected, changing our perspective on how to deal with high consequence - low probability events (Stein and Okal, 2007). The first global scale tsunami hazard and exposure assessment was conducted for the UN-ISDR Global Assessment Report 2009 (GAR, 2009), and is also summarized by Løvholt et al. (2012a). GAR 2009 focussed on tsunami exposure due to low probability-high consequence events. Emphasis was put on developing countries as certain regions were omitted or not fully covered.

Here, the methodology and results for the GAR 2013 report are outlined. The recent 2011 Tohoku earthquake and tsunami lead to an increased focus on impact of natural hazards on critical facilities. This is also reflected in the objectives of the GAR 2013 report. This event, among others, has led to the following objectives for the GAR 2013 report:

- Owing to the need for a global analysis, the proposed method for quantifying the tsunami hazard is based on simplifications and approximations, and is focusing on overall trends rather than details. The results of the study are hence a first-pass assessment of the tsunami hazard and population exposure.
- A primary objective in GAR 2013 is to provide a more complete coverage of earthquake tsunami sources globally to properly account for the exposure of population and critical facilities also in the industrialized countries in addition to previous focus regions from GAR 2009. Emphasis has been given to near field effects of tsunamis as these generally provide the larger run-up and shorter evacuation times.
- In order to obtain better statistics, a closer and more systematic sampling of offshore control points for run-up and exposure calculations has been conducted.
- Earthquakes account for more than 80% of the tsunamis globally and therefore the focus of GAR 2013 is limited to earthquake induced tsunamis. Tsunamis caused by landslides, rock slides, and volcanoes are not included in this study.
- The study focuses on tsunamis caused by large earthquakes only, as the largest events contribute more to the risk than the smaller events (Nadim and Glade, 2006).
- The design of new earthquake scenarios for GAR 2013 is constrained by the subduction zone convergence rate, conservatively assuming fault locking over 500 years. This gives a more formalized procedure for selecting the scenario earthquakes, as detailed below.

2 Methodology

The objective is to produce global hazard maps and statistics of the exposure of elements at risk. The present report focuses on the population exposure and critical facilities. The tsunami inundation and exposure are obtained for a single return period of 500 years (close to a 10% exceedence probability in 50 years). Reliable estimates of the hazard at such large return periods are not easily established, particularly given the geographical extent of the problem and various sources of error and uncertainty. Hence, the return period is indicative to the order of magnitude only. Exposed areas are obtained by intersecting the modelled inundation with population density maps (Landsat, 2007) and economical values located in tsunami-prone areas in order to compute the exposure. To obtain such maps, scenario simulations are widely applied, to a large degree adopting the scenario methodology applied by Løvholt et al. (2012a), partly replacing previous results from GAR 2009, but also expanding the study area. Literature results are retained from GAR 2009 for New Zealand (Berryman et al., 2005) and Kamchatka (Kaistrenko et al., 2003), similarly earthquake scenario simulations covering the subduction zones offshore South America and along the Philippine and Manila trenches. Furthermore, results applied using probabilistic methods (PTHA, see e.g. Geist and Parsons, 2006; Thio et al., 2010) are used for certain areas. The various methods are briefly described below.

2.1 Design of the earthquake scenarios

The considered earthquake scenarios are confined to those with the potential for tsunami generation due to co-seismic dip-slip motion. A compilation of all the scenarios are given in Figure 1. New scenarios cover eastern Indonesia, the Philippine trench and the northern Manila trench (Figure 2), northwards along the Ryukyu trench, the Nankai trough to the Japan trench (Figure 3). In the eastern Pacific new scenarios along the Aleutian trench and Cascadia trenches are provided (Figure 4). Previous scenarios from GAR 2009 for South America and new scenarios covering the Puerto Rico trench are depicted in Figure 5. For Europe potential earthquake scenarios offshore Portugal and the Eastern Mediterranean, including Sicily, the Adriatic Sea, and the Hellenic Arc are provided (Figure 6). A final set of scenarios are provided for the Makran trench south of Pakistan and Iran (Figure 7). Results for the South and South East Asia and the South West Pacific were obtained by the more elaborate PTHA method described below. The PTHA method combines relatively small unit sources for a range of subduction zones, these are not displayed below.

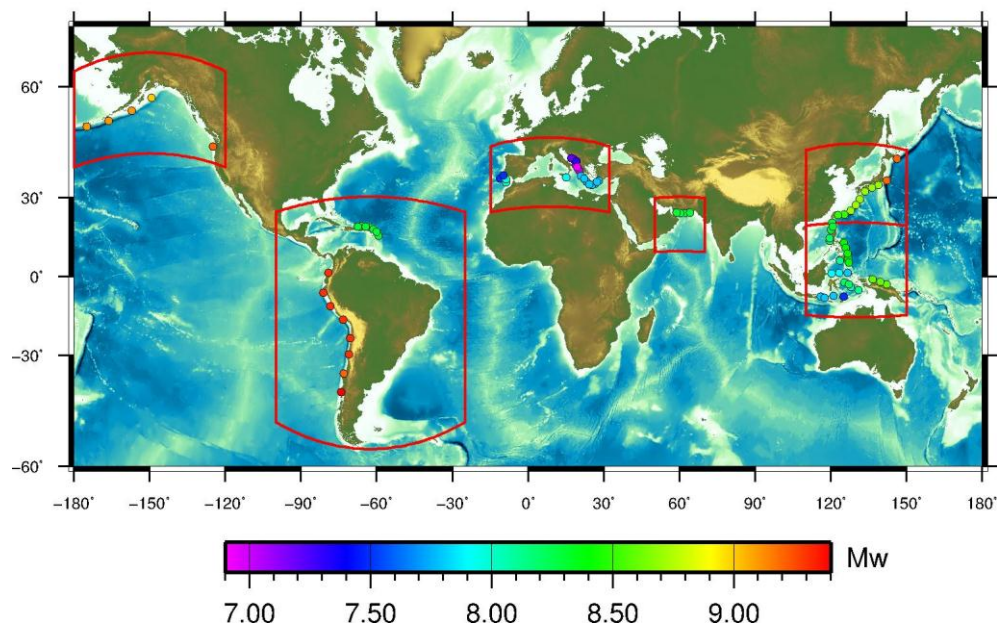


Figure 1: Overview of the locations of the new employed scenarios in the present study. The red boxes depict areas presented below. The coloured dots represent the moment magnitudes and scenario locations. It is noted that for the Indian Ocean and south western Pacific, the PTHA is employed. The many PTHA unit sources are not displayed.

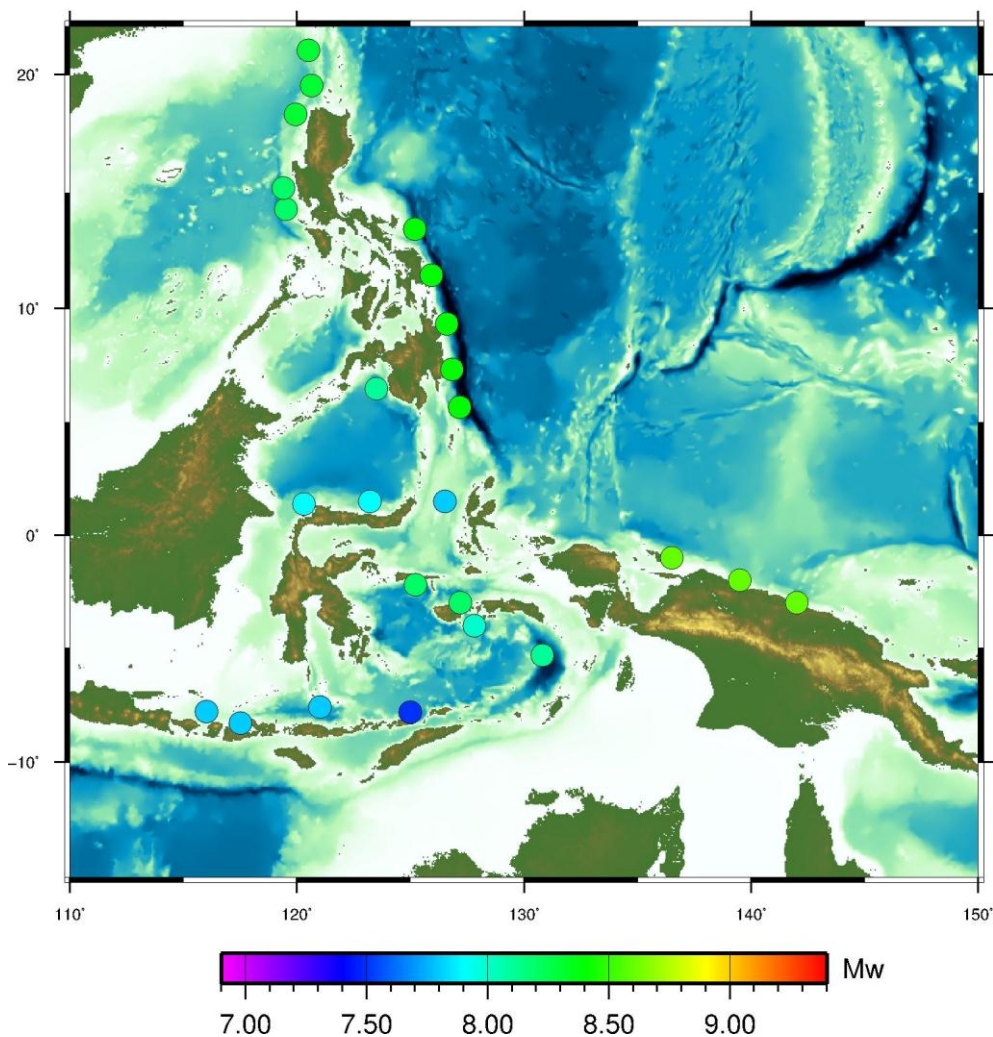


Figure 2: Scenarios located in eastern Indonesia, the Philippines and New Guinea.

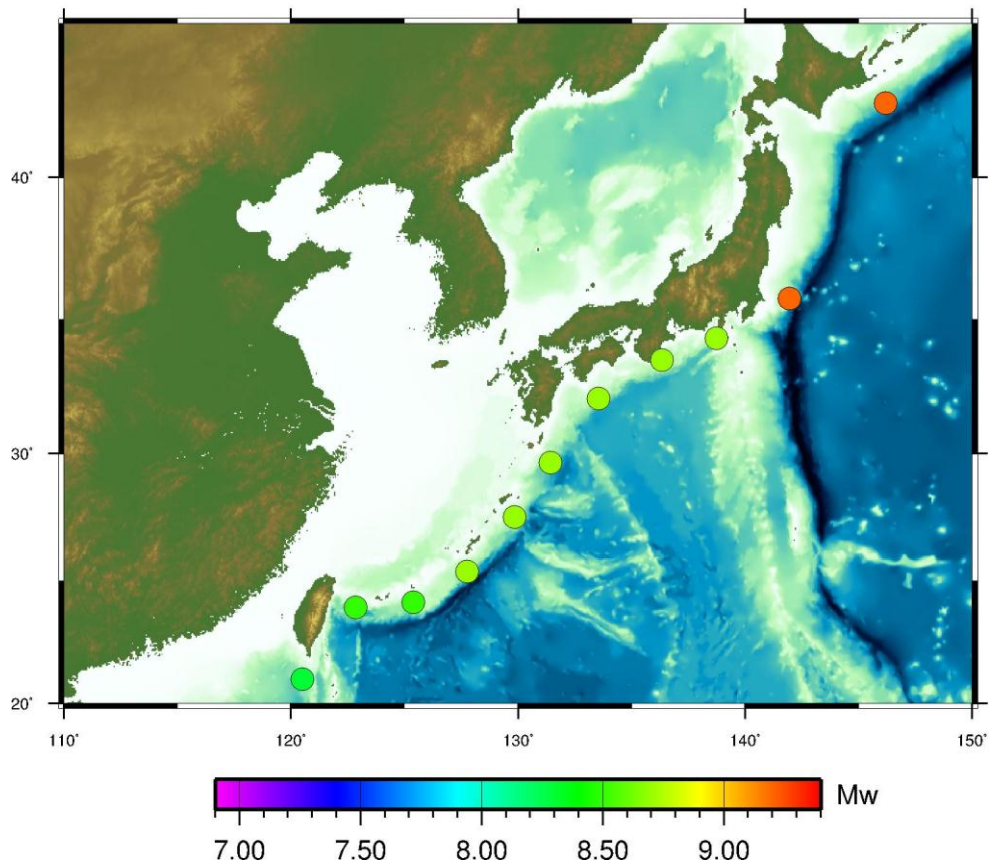


Figure 3: Megathrust scenarios located along the Ryukyu trench, the Nankai trough, and the Japan trench.

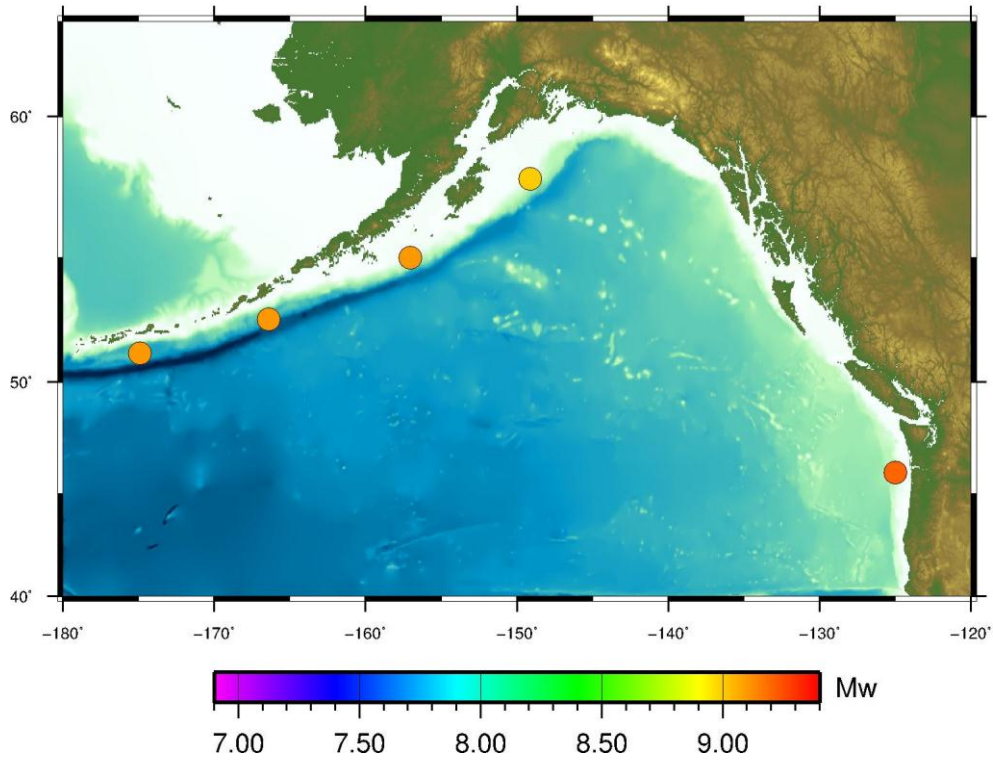


Figure 4: Megathrust scenarios located along the Aleutian and Cascadia subduction zones.

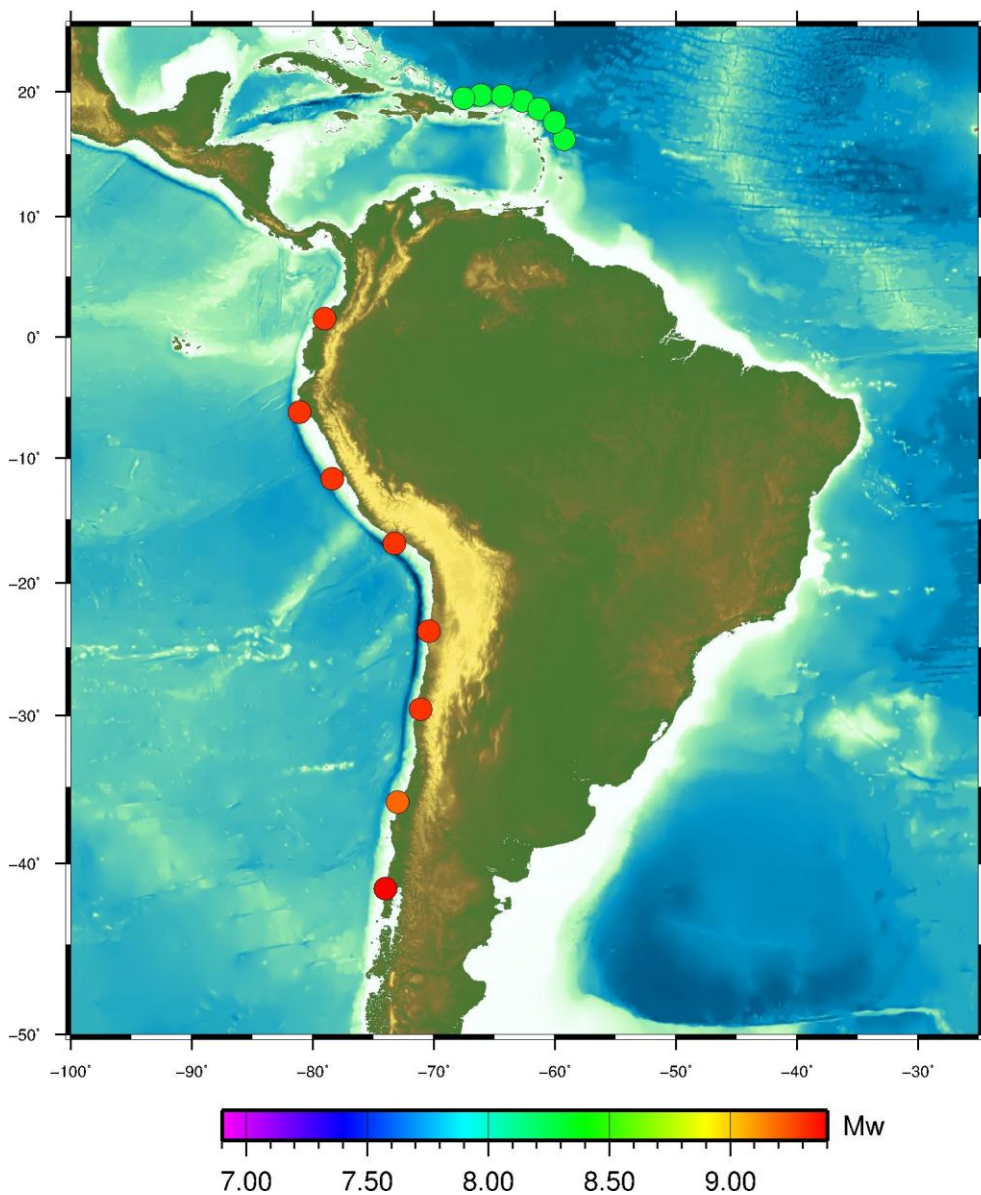


Figure 5: Scenarios located along subduction zones offshore South America and the Caribbean.

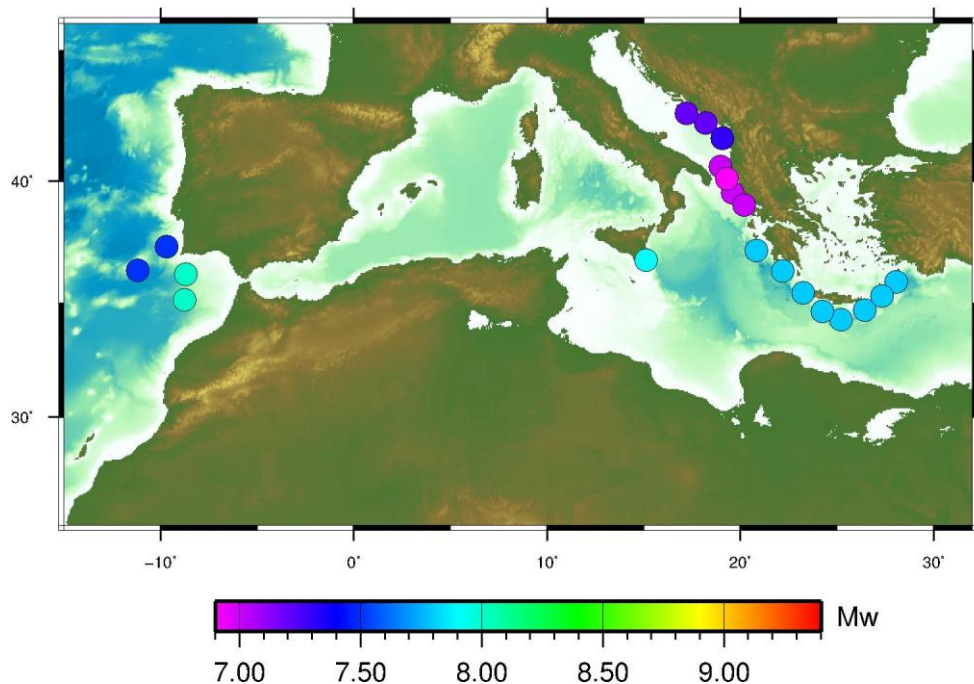


Figure 6: Scenarios offshore Portugal and in the eastern Mediterranean. Note that the scenarios offshore Portugal is related to larger return periods and uncertainties with respect to focal mechanisms than the other scenarios.

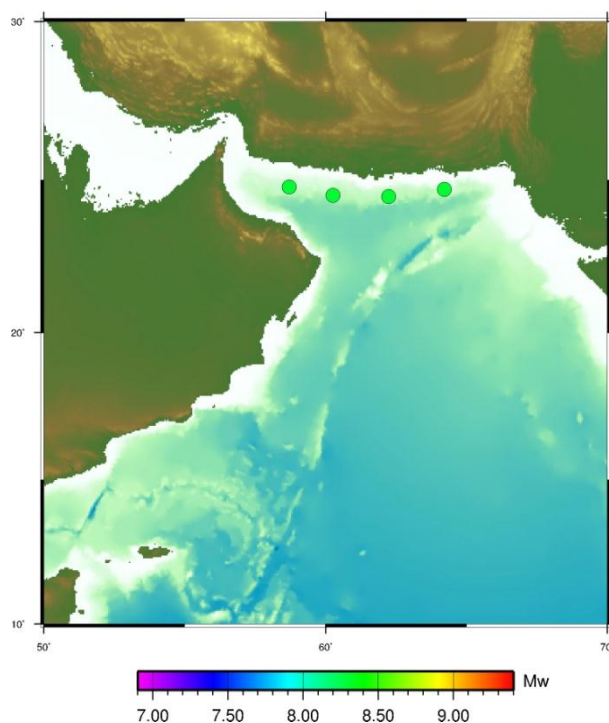


Figure 7: Makran trench scenarios.

For the scenario earthquakes, earthquake faults of uniform width, length and slip are established, and in turn converted to seabed displacement using the standard analytical formula of Okada (1985). Smoothing due to the hydrodynamic response from the seabed dislocation is based on the formula of Kajiura (1963). For the subduction zone earthquakes where slip rates were obtained, the new scenarios were constructed assuming fault locking over 500 years. Convergence rates obtained from Bird (2003) are used. By using the scaling relations from Blaser et al. (2010), related magnitudes were found. By making assumptions on the fault shear strengths, related fault lengths and widths were in turn derived from the scaling. Typically the shear strengths were in the range of 20-40 GPa. Altogether this gives relatively conservative estimates for the scenario earthquakes. However, as discussed below, there are several other assumptions in the overall methodology that are non-conservative.

In certain areas where tectonics are more complex the slip rates and fault geometry are less easily obtained. Here, fault parameters are reproduced as accurately as possible from literature. As a consequence, the return periods are also less accurate. Yet, the return periods for these scenarios are assumed to be fairly similar to those originating from subduction zones. Literature data were used for Sicily (Tinti et al., 2012), the Adriatic Sea (Tiberti et al., 2008), eastern Indonesia (Løvholt et al., 2012b), and Cascadia (González et al., 2009). The scenarios offshore Portugal is motivated from the recent studies of Matias et al., (2013), aiming at a 500 year return period. It is noted that scenarios of similar magnitude of the 1755 earthquake and tsunami would imply return periods of several thousand years according to Matias et al., (2013). The scenarios offshore Portugal have different orientations, which reflect the uncertainty due to present lack of knowledge of the most likely focal mechanisms for megathrusts in this region.

2.2 Wave propagation modelling

Near source and regional tsunami propagation are modelled using a linear dispersive wave model GloBouss (Pedersen and Løvholt, 2008; Løvholt et al., 2010), on publicly available ETOPO1 grids. For convergence, the grids are refined to the desired resolution by bi-linear interpolation. The maximum water level obtained from the time series at the control points is used to compute the further amplification to the shoreline as described in Section 2.4 of the surface elevation are extracted at near shore control points, and in turn the maximum water level is used. Totally over 10000 control points are applied, with an approximately spacing of 20 – 50 km. The control points are extracted automatically by a contouring algorithm (GMT, 2011) at a small reference depth of 50 meters. Inside the tsunami model the depth in the control point may deviate from the reference depth, so the surface elevation is normalized to 50 m by using Greens' law.

2.3 Employed Probabilistic Tsunami Hazard Assessment method

The Probabilistic Tsunami Hazard Assessment (PTHA) approach describes the probability of exceedence for a given tsunami metric, and is derived from the well established method of Probabilistic Seismic Hazard Assessment (Cornell, 1968) but adapted to account for tsunami propagation. Relatively recent studies have applied the PTHA method to different regions, e.g. Geist and Parsons (2006) Annaka et al. (2007), Burbidge et al. (2008), Parsons and Geist (2009), and Thio et al. (2010). A short description of the employed PTHA method follows here, for a more complete description we refer to Horspool et al., (in prep).

The PTHA framework can be summarized as:

- Define tsunami sources (earthquake faults) to be included in the analysis.
- For each source discretize the fault into smaller sub-faults.
- For each source create a synthetic earthquake catalogue based on a recurrence model of choice (e.g. Gutenberg-Richter or Characteristic), which has probabilities associated with each earthquake.
- For each sub fault, calculate the unit seafloor deformation and propagate the tsunami from source to the control points at the reference depth.
- For each event in the catalogue, estimate the maximum water level at the near shore control point by summing the waves from all the individual sub faults that make up that event, and then scale by the amount of slip for that event.
- Combine the maximum water level from all sources to estimate the probability of exceedence.

The PTHA method was employed for the Indian Ocean and the South West Pacific. Tsunami megathrust sources around the western and northern Pacific Ocean, the Makran subduction, and the Sunda Arc were used. The subduction zone geometry and recurrence rates were taken from the PTHA for Australia (see i.e. Burbidge et al., 2008), which uses plate velocity vectors from GPS data to estimate the magnitude frequency distribution assuming full coupling on the plate interface. Sub faults for local crustal sources are 20km x 10km, whereas sub faults that are distant only are 100km x 50km.

In deep water the tsunami is linear, meaning that any tsunami can be constructed by the summation of the responses from the sub faults. Hence, the simulations are only carried out ones for the sub faults, and the hazard is determined by superpositioning. In the PTHA a linear finite difference model allowing for nesting formulated in geographical coordinates (Satake, 1995) is used for the simulation of the tsunami propagation for the unit sources. As for the worst case scenario simulations the maximum water elevation was extracted at the 50 m reference depth.

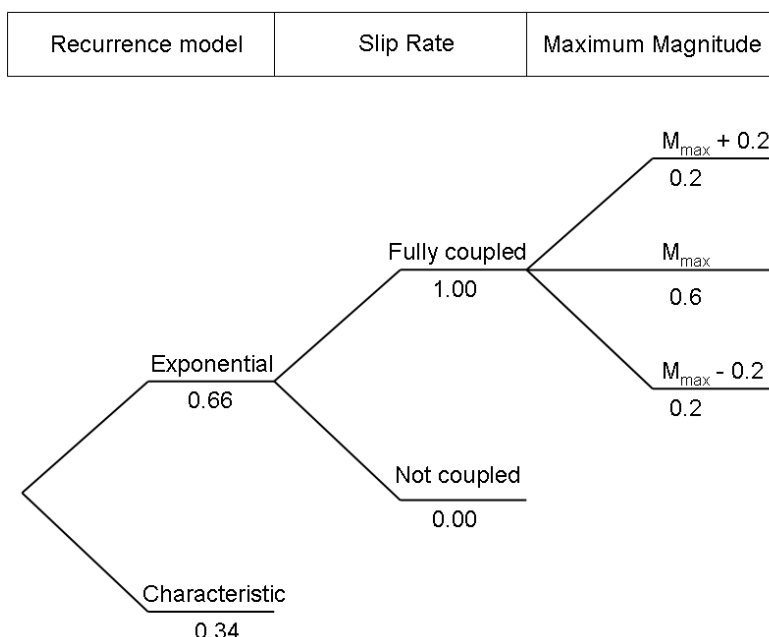


Figure 8. Outline of PTHA logic tree.

Sources of epistemic uncertainty (uncertainties due to lack of knowledge) that are included in the PTHA are slip rate, earthquake recurrence model type, and maximum magnitude (Figure 8). Maximum magnitudes are constrained by scaling laws (Blaser et al., 2010). The maximum magnitude from the mean of the scaling laws is given a weighting of 0.6, and two alternative maximum magnitudes that are +0.2 magnitude units and -0.2 magnitude units from the best estimate, are given a weighting of 0.2. For each source, a truncated Gutenberg-Richter Magnitude Frequency Distribution (MFD) was given a weighting of 0.66 and a Characteristic Earthquake distribution was given a weighting of 0.34. A b-value of 1.0 is used for both MFD's. Main sources of aleatory uncertainty (inherent uncertainty) in the PTHA come from modelling uncertainties in source geometry, and random slip. The aleatory uncertainty was accounted for by summing up different variances from model errors, fault dip, and random fault slip. The uncertainties in dip and random slip were obtained from Monte Carlo simulations by varying the dip angle and employing the different slip realizations, respectively. Aleatory uncertainties were included by integrating across probability density functions.

Combining all the information from the sources and logic trees, a synthetic catalogue is generated which represents the full integration over earthquake magnitudes, locations and sources for every logic tree branch. The catalogue was generated by iterating through each magnitude in the MFD, and calculating the rupture dimensions using the scaling laws (Blaser et al., 2010). The rupture is then iteratively moved across the fault one sub fault at a time until that magnitude has occurred on every possible location within the fault

dimensions. For M7.0 earthquakes on the subduction interface, the rupture dimensions are equal to one sub fault; therefore the number of ruptures would be equivalent to the number of sub faults. The maximum magnitude earthquake would occur once and rupture the whole fault if scaling laws have been used to constrain the maximum magnitude. This iterative process ensures that all magnitudes could occur at any possible location on the fault plane. For each event the probability of that magnitude was then weighted by one over the number of earthquakes represented by that magnitude. This ensures that the sum of the events of the same magnitude equals the annual probability of one event of that magnitude.

For each event in the synthetic catalogue, the tsunami hazard is calculated at each control point along the coast by summing the contributions from the sub faults that make up that event, and by scaling the tsunami height by the event slip. For each site, this results in a list of tsunami heights and associated annual probabilities. For a coherent description of the hazard compared to the worst case scenario simulations, maximum surface elevation from the PTHA for a return period of 500 years is given at near shore control points at the reference depth of 50 m. The further amplification to run-up is accounted for using the amplification factor method (Section 2.4). The present model assumes a Poisson process where earthquakes are independent and occur at a fixed rate over time.

2.4 Run-up estimation and inundation mapping using amplification factors

To estimate tsunami run-up globally refined numerical inundation simulations are too time consuming. A faster procedure is to relate the nearshore surface elevations to the maximum shoreline water levels by using a set of amplification factors based on the parameters of the incident wave and the bathymetric slope. This procedure was developed for GAR 2009, and is described and validated in detail by Løvholt et al. (2012a), and only a part of the procedure is reviewed here.

The procedure is sketched in Figure 9. A range of different earthquake fault parameters are used to provide the set of initial conditions. These include the earthquake fault width (50, 100, 150, 200 km), and dip angle (5, 15, 20, 30 degrees), as well as inverting the polarity of the tsunami (leading trough or crest). The plane wave simulations are all run on idealized plane bathymetric configurations (see Løvholt et al., 2012a) where the shelf is broken up into two linear segments. From the plane wave simulations, factors for amplification that relate the surface elevation at time series gauges located at water depths of 50 m to the maximum shoreline water level are computed and stored in lookup tables. To determine the amplification factors along the idealized bathymetric profiles we apply a linear hydrostatic plane wave model. For smaller islands the plane wave assumption is severely violated, a 2HD model (GloBouss) must be applied. Both models apply a no-flux boundary condition at the shoreline leading to a doubling of surface elevation due to reflection. Although the

models do not include dry land inundation, the surface elevation on the boundary close to the shoreline (at 0.5 m water depth) with a no-flux condition yields a good approximation. For long non-breaking waves, the linear solution for the run-up height at the shoreline and the non-linear solution for the run-up height on land are identical (Carrier and Greenspan, 1958). The validation of procedure is presented in Løvholt et al. (2012a). Based on Pedersen, (2011), we may further assume that the procedure should also provide reasonably accurate results for waves of moderately oblique incidence. For reviews of different methods for run-up estimation, see Synolakis et al., (2007), Pedersen (2008), and Løvholt et al., (2013).

To assign an amplification factor, an idealized bathymetric profile is manually assigned to each point. To estimate the maximum shoreline water level from the offshore time series gauges in a tsunami simulation, the amplification factor for a set of parameters is extracted from the lookup tables and in turn multiplied with the maximum surface elevation measured at the time series gauges.

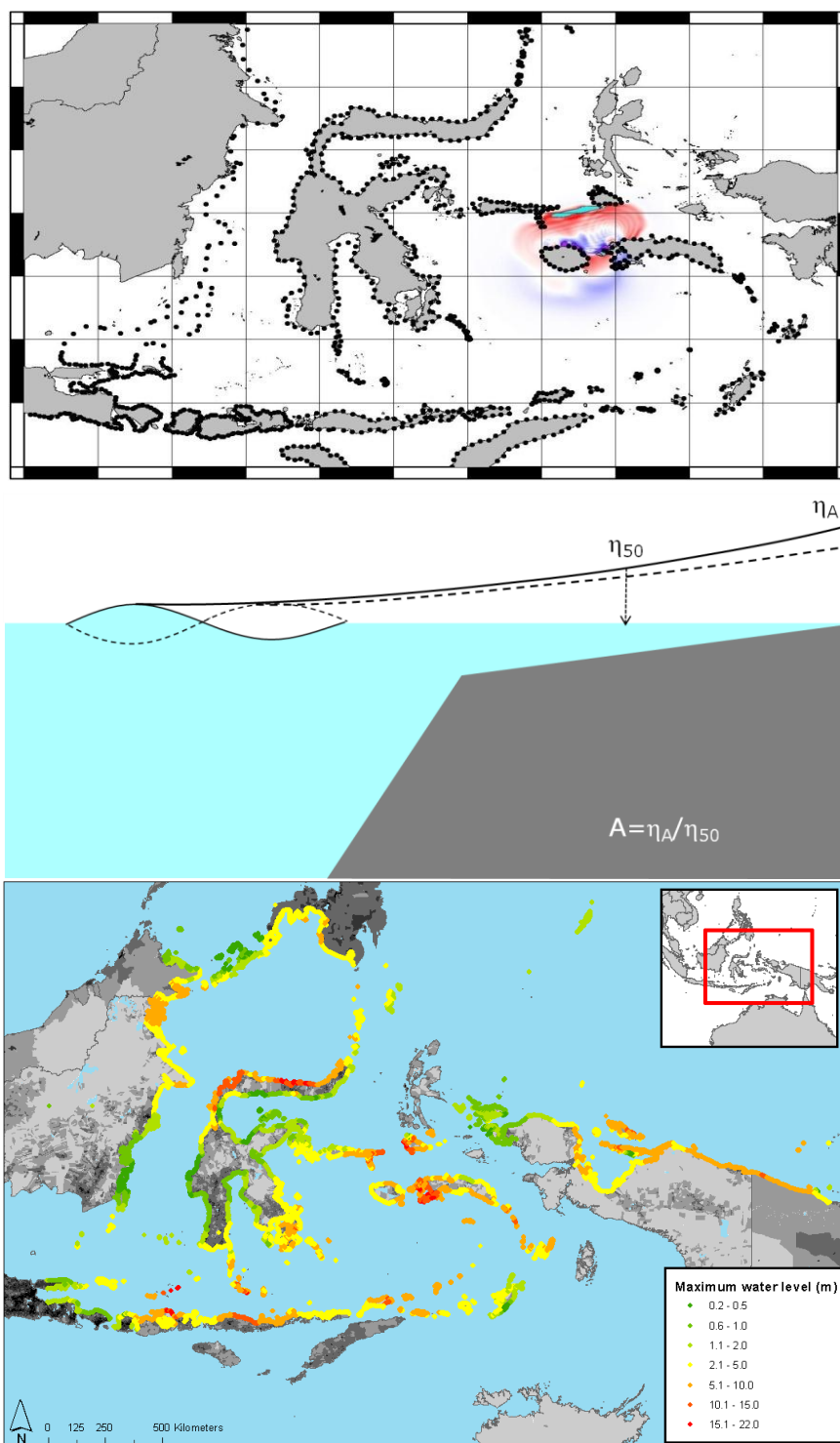


Figure 9: Principles of the amplification factor method. Upper panel, regional tsunami simulation and locations of the time series gauges at the reference depth contour. Mid panel, sketch of an idealized bathymetric profile. The amplification factor is defined as the ratio between the water surface elevation at the shoreline over the water surface elevation at 50 m water depth. Lower panel, maximum shoreline water level obtained from superimposing results from a series of simulations.

2.5 Inundation mapping and exposure

Based on the maximum shoreline water levels, rough inundation maps were computed to count the population exposed to the tsunami. The inundated area was computed by first interpolating the water levels at the shoreline. An inverse distance weighted method was used to extrapolate the water elevations at the shoreline to the topographic contour maps. For the topographic data, the SRTM dataset was used. However, it turned out that for some very flat near shore locations, the inundation distance could be unreasonably high. To limit the inundation, a crude formula taking into account the head loss due to bottom friction was used. We represent the wave load at the shoreline by a constant surface elevation η and choose a friction coefficient $f=10^{-2}$. This friction is relatively high, slightly counterbalancing the conservative assumption of fault locking, yet providing reasonable inundation distances compared to real events. By assuming a quadratic friction law and a constant drop of hydraulic head loss along the inundation path, a simple formula for the maximum inundation distance L_{max} was obtained, proportional to the ratio of the surface elevation over the friction:

$$L_{max} < \frac{\eta}{f}$$

The inundated areas represent 500 year return period hazard maps. The inundation maps are then overlaid on population exposure data (Landscan, 2007) and critical facility data for nuclear power plants (database provided by UNEP-GRID) and airports (<http://www.ourairports.com/data/>) to provide country wise and global statistics of the 500 year return period exposure. The total population exposure is found by integrating the Landscan data over the inundated area. Generally, the predicted inundation line intersects a Landscan grid cell. In this case, the exposed population is taken as the cell population times the inundated cell area over the total Landscan cell area. Only airports defined as medium and large were included in the statistics. Due to the limited accuracy of the inundation maps, three different categories were used in the exposure calculations for the critical facilities in order to take into account model uncertainty. The first category (Cat1) is a facility located in a potential inundated area. The second category (Cat2) is a facility located less than 1 km from the shoreline defined by the SRTM dataset. The third category (Cat 3) is a facility not exposed or not in area covered by this study.

3 Results

Using GloBouss, the tsunami propagation was simulated for the 80 scenarios depicted in Figure 1. Examples of the simulated maximum water levels are depicted in Figure 10 through Figure 13. For each scenario, the maximum water level is found at the near shore control points, and the run-up is estimated using the amplification factors. As the control points are common for all scenarios, the largest of the maximum water levels are extracted from all scenario simulations. For the areas covered by the PTHA method, the exceedence amplitude for a return period of 500 years is reported.

Figure 14 shows the distribution of tsunami hazard globally from earthquake induced tsunamis. The analysis shows that populous Asian countries, most prominently Japan, but also China and Indonesia account for a large absolute number of people living in tsunami prone areas (Figure 15). This is due to the combination of large hazard and dense population. A similar hazard is found along the US and South American coastlines, but here the total exposure are smaller. In relative exposure, smaller countries like Macau and the Maldives are among the highest ranked countries. In these countries, a higher amount of the total population is exposed to tsunamis. Since tsunamis have a low probability of occurrence, Figure 15 provides the number of people living in tsunami-prone areas and not the average yearly exposure as provided for other hazards. Close-up of some locations are found in Figure 16, where examples of critical facilities such as nuclear power plants as well as airports close to or inside the tsunami hazard zone are given.

Examples of critical facilities that may be inundated by tsunamis include nuclear reactors and airports. Categories 1 and 2 are included in the statistics for both kinds of facilities. Figure 17 shows countries having nuclear power plants and reactors close to or within the inundated area. Japan has the largest number of nuclear power plants within the inundated area (7). When the nuclear power plants close (less than 1 km) to the shoreline is included, the United States has the largest total number (13). In Figure 18 the countries with the largest number of airports inside and close to the tsunami hazard zone are listed. Japan has the largest number of airports inside the hazard zone (24), while the United States have the largest total number including also those close the hazard zone (58). In certain areas such as the eastern United States and the United Kingdom, landslide induced tsunamis may constitute an additional significant threat towards critical facilities, but these tsunami sources are not included in the current statistics even though near shore critical facilities may in general be exposed to this additional threat.

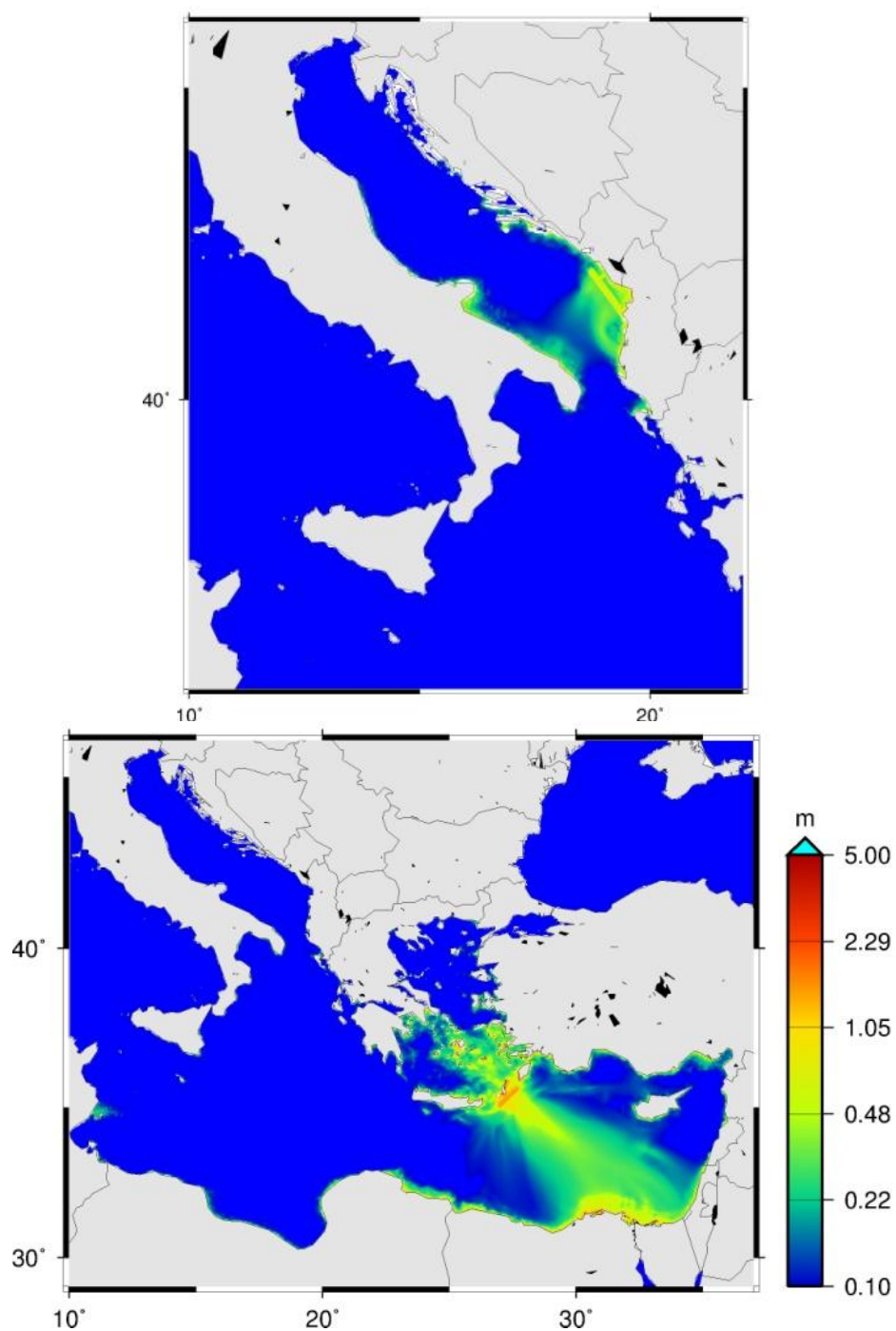


Figure 10: Examples of simulated maximum water levels from two scenarios. Upper panel, example from the Adriatic Sea; lower panel, example from the Hellenic Arc. The colorbars indicate the maximum water level in meters.

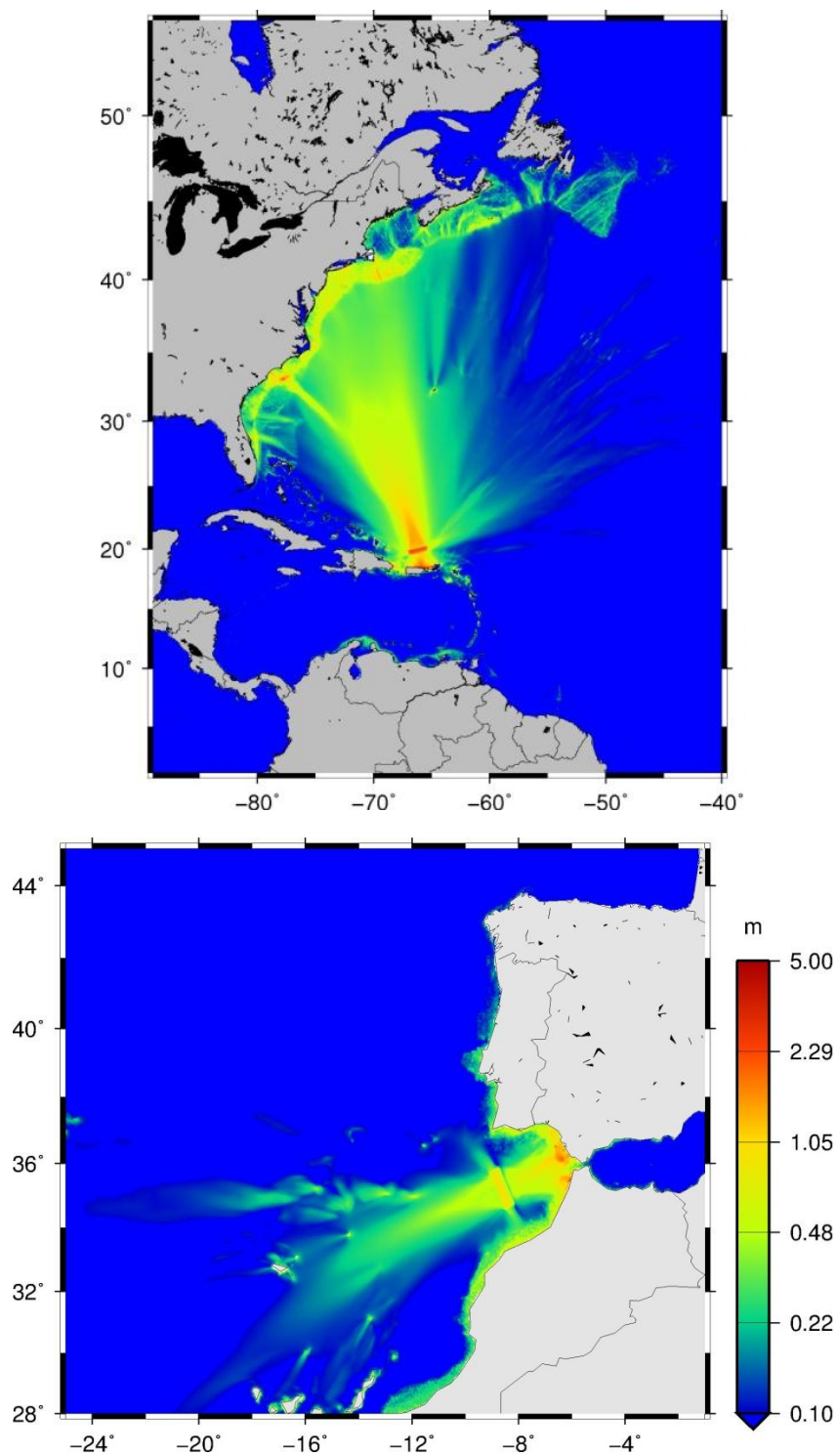


Figure 11. Examples of simulated maximum water levels from two scenarios. Upper panel, example from the Puerto Rico trench; lower panel, example from offshore Portugal. The colorbars indicate the maximum water level in meters.

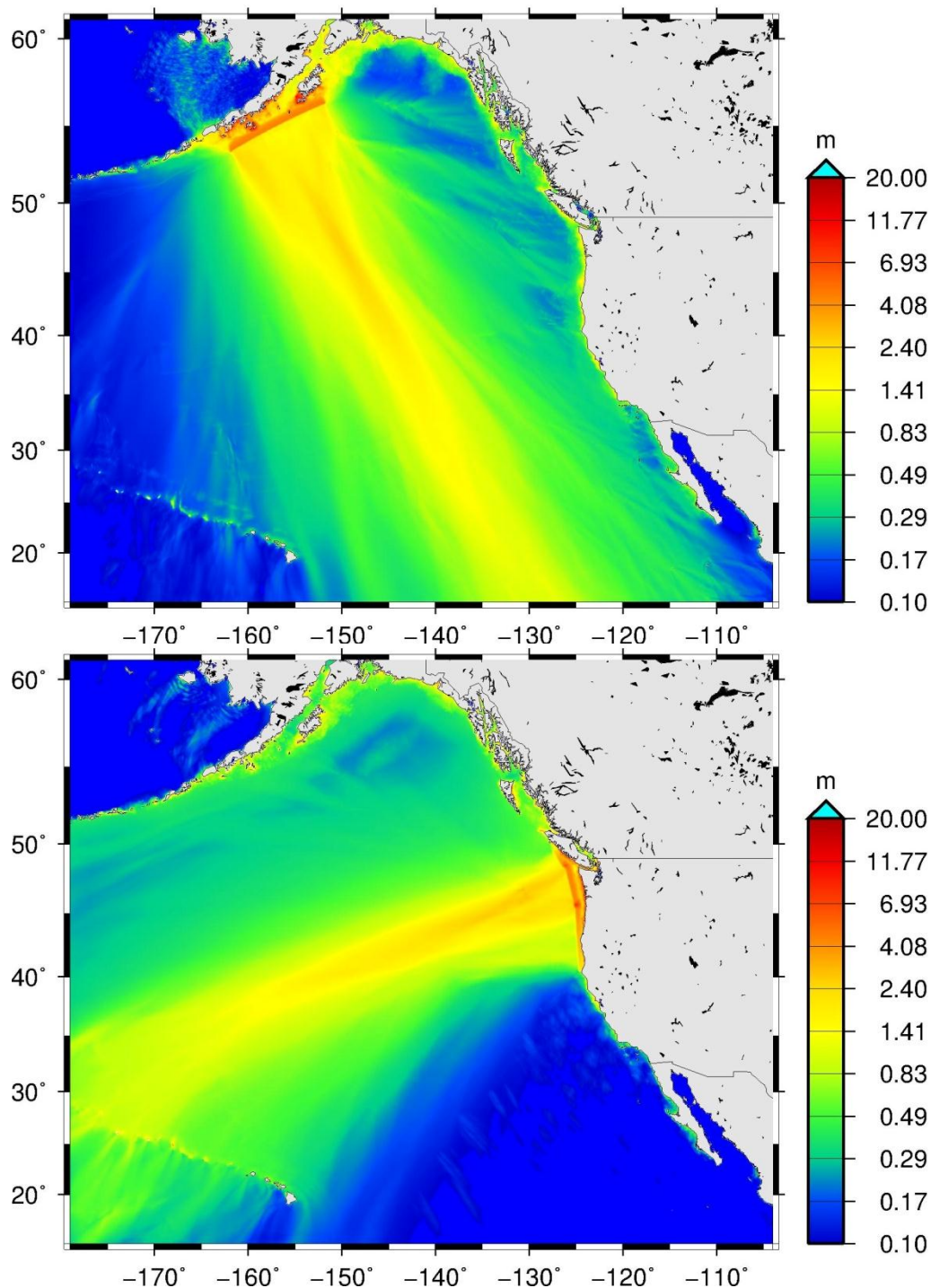


Figure 12. Examples of simulated maximum water levels from two scenarios. Upper panel, example from Aleutian trench; lower panel, example from the Cascadia subduction zone. The colorbars indicate the maximum water level in meters.

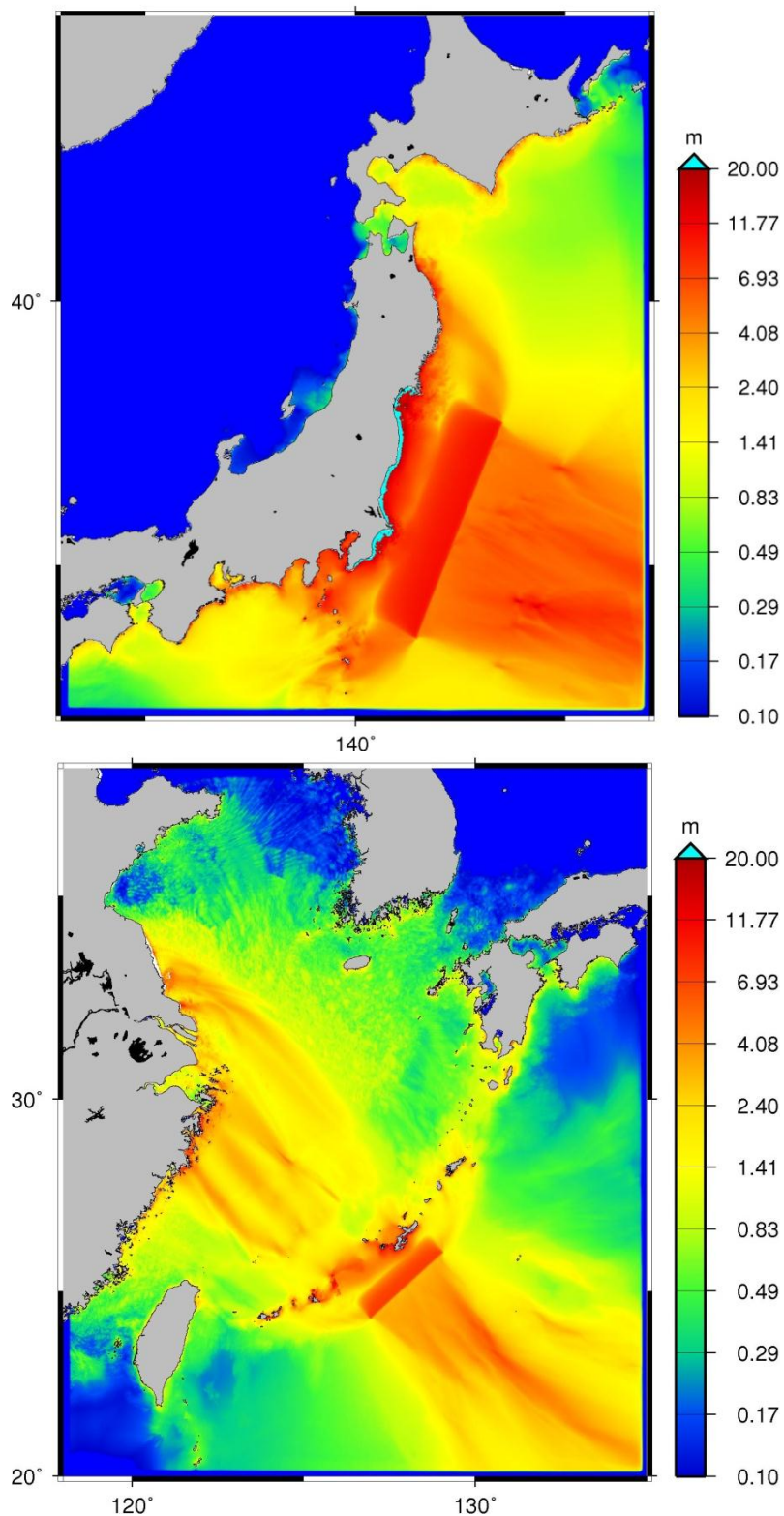


Figure 13. Examples of simulated maximum water levels from two scenarios. Upper panel, example from the Japan trench; lower panel, example from the Ryukyu trench. The colorbars indicate the maximum water level in meters.

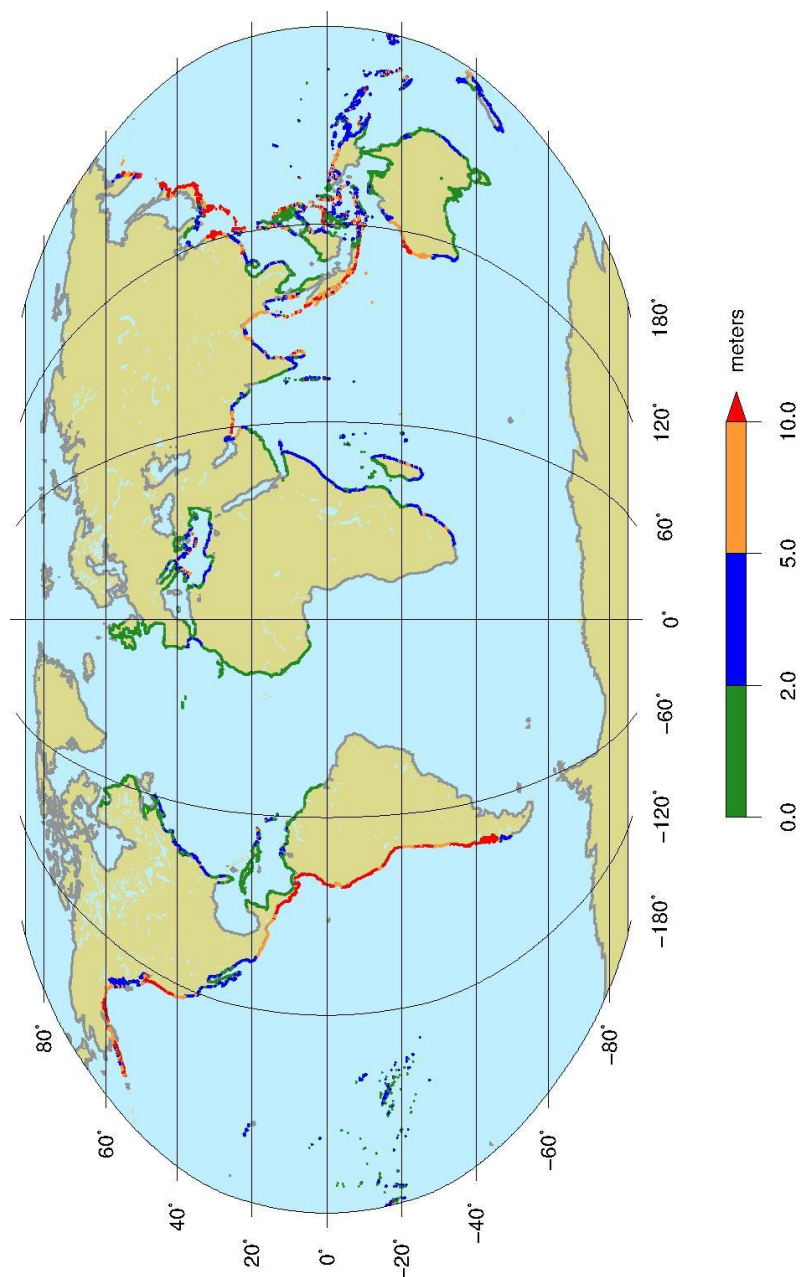


Figure 14: Global tsunami hazard due to earthquakes for a 500 year return period. The color bar gives the maximum shore line water level in meters.

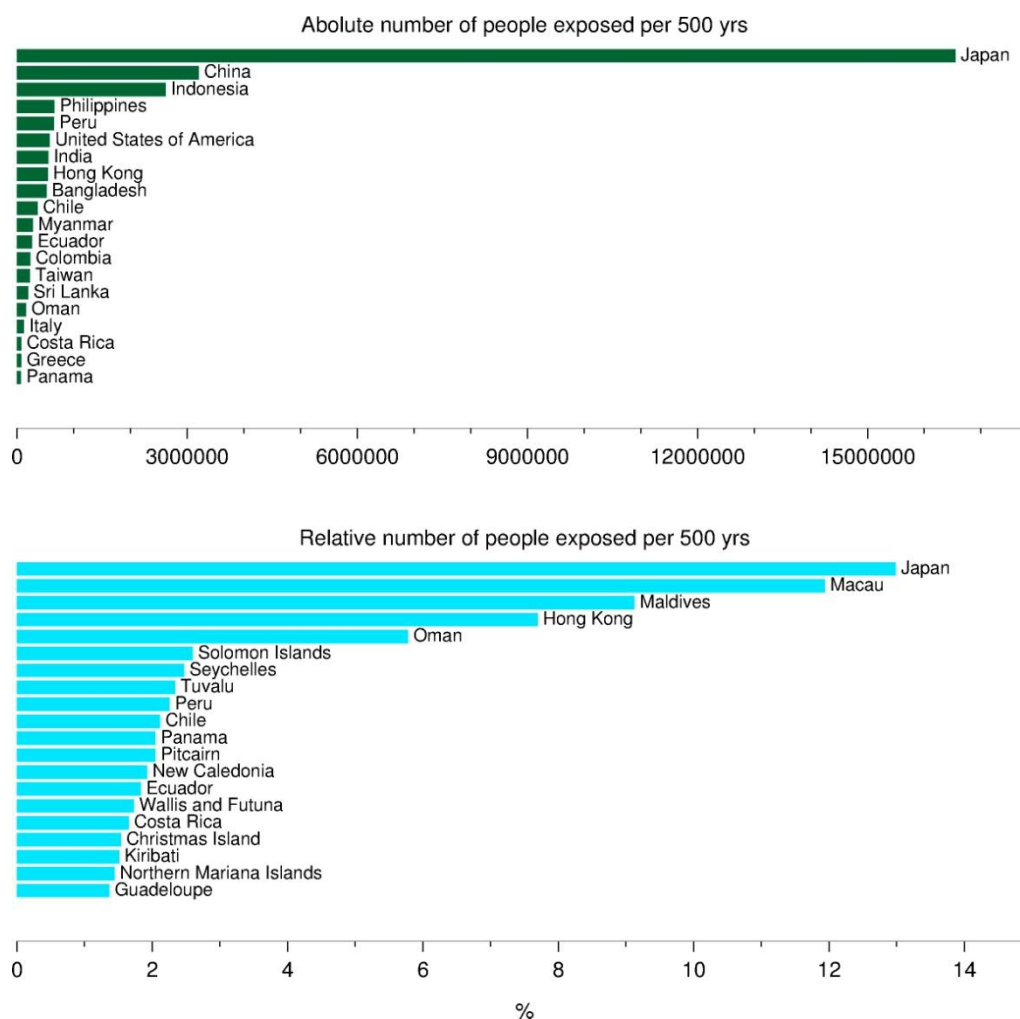


Figure 15: Number of people living in areas potentially affected by tsunamis for a 500 year return period. The number of exposed persons divided by the total population in each country is given in percent in the lower panel.

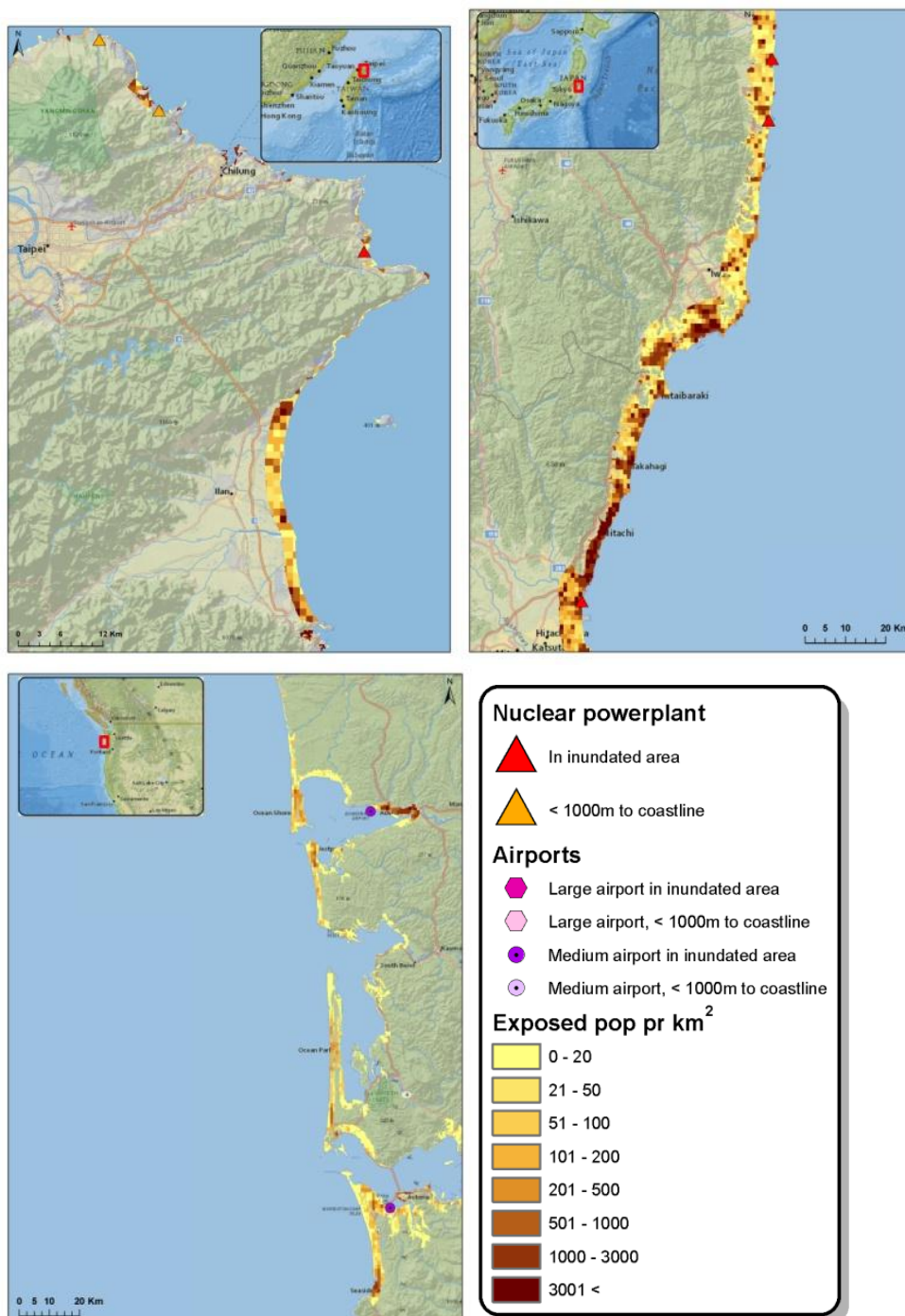


Figure 16: Examples of tsunami exposure at northern Taiwan, eastern Japan, and western US coastline for a 500 year return period. Both population density and critical facility exposure are depicted.

Absolute number of nuclear powerplants inside (red) and close (orange) the tsunami hazard zones

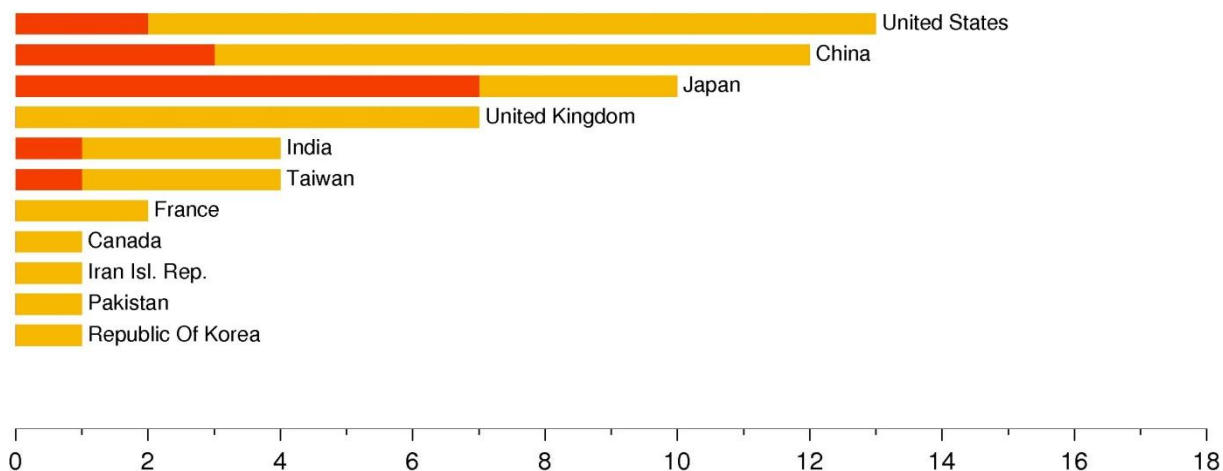


Figure 17: Nuclear power plants close to or inside the tsunami inundation zone for a 500 year return period. The red color indicates number of nuclear power plants inside the tsunami hazard zone (Cat 1), while the orange color indicates the number of power plants closer than 1000 m to the tsunami inundation zone (Cat 2).

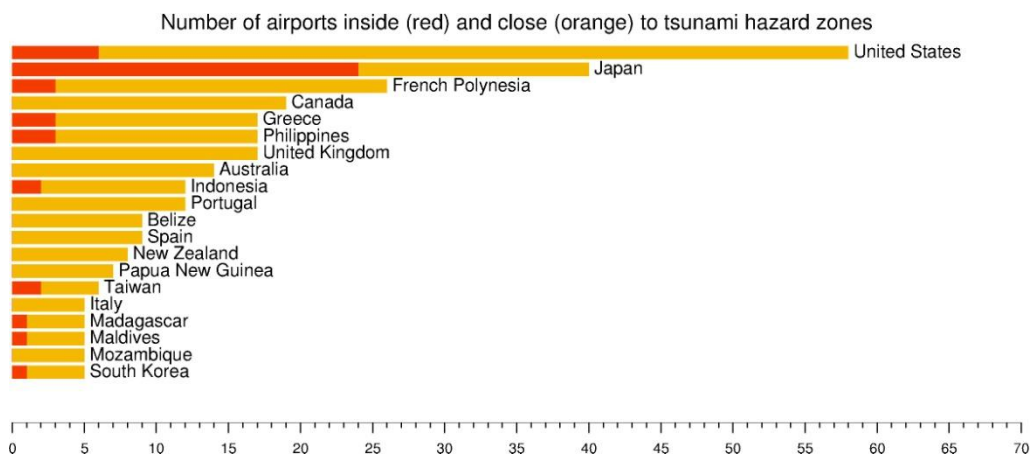


Figure 18: Number of airports (large or medium) for (Cat 1, red) or closer than 1000 m (Cat 2, orange) to the tsunami inundation zone for a 500 year return period.

4 Limitations, sources of error and look ahead

Below, the different limitations of the study are outlined. These partly address sources of error in the analysis, and partly the missing parts in the risk quantification. It is stressed that the results of the present analysis is deterministic, and although there are uncertainties related to the analysis, these are presently not quantified. Future updates of GAR will apply a probabilistic analysis (based on the PTHA method), and hence uncertainties will be addressed more quantitatively.

4.1 Return periods

The largest and most destructive tsunami events like the 2004 Indian Ocean and 2011 Tohoku tsunami are generally posing larger risk to human lives than the smaller and more frequent events. For this first pass analysis, the tsunami hazard maps are focussing on extreme events only, that is, tsunamis generated by large earthquakes of return periods of approximately 500 years. It is noted that establishing the size of infrequently occurring earthquakes is uncertain due to the lack of a reliable long record. Hence, the return periods for the future tsunamis are not to be interpreted as precise estimates. We also remark that the assumption of a “memory free” fault and fault locking is conservative, as areas where recent large earthquakes have occurred may actually have a lower probability than the ones interpreted here. Still, due to the nature of the recent large earthquakes causing major tsunamis, it has been interpreted as necessary to provide conservative estimates of the scenario earthquake in order not to underestimate the hazard and risk.

Although earthquakes with a return period of roughly 500 years are often expected to provide the largest contribution to tsunami risk, earthquakes with both higher and smaller probabilities will contribute strongly. Megathrusts with return periods exceeding thousands of years, may imply much stronger tsunami sources than those provided here. In certain areas, such as for instance offshore Portugal, Spain, and Morocco, these may even be the risk driving events. Providing a range of tsunami return periods will therefore be necessary to more accurately estimate exposure and to quantify the risk.

4.2 Non-seismic sources

It should also be noted that tsunamis generated by volcanoes, submarine landslides, rock slides and smaller earthquakes are not addressed in the present study. Non-seismic sources contribute to the generation of about one fifth of all tsunamis globally, and there are several examples of such tsunamis causing devastation, a recent example is the 1998 Papua New Guinea tsunami caused by a submarine landslide, killing 2182 people (source, <http://www.emdat.be>). In areas like eastern Indonesia (Løvholt et al., 2012b) and the Caribbean (Harbitz et al., 2012) tsunamis due to landslides and volcanoes are relatively

more frequent, and contribute to a significant portion of the risk. It has also recently been claimed that large run-up in northern Japan following the 2011 Tohoku tsunami was induced by a huge submarine slump (Grilli et al., 2012). Unlike earthquakes, landslides are not constrained to the major subduction zones and may strike more surprisingly. Due to their source characteristics, they may generate larger run-up locally compared to earthquakes, but are generally less dangerous for the far field propagation (for a discussion of their hazard, see e.g. Harbitz et al., 2013). However, addressing their return periods is difficult.

4.3 Interpretation of hazard maps and population exposure

Due to the extensive task of covering the whole world, emphasis is given to producing regional hazard maps and numbers for the exposure. The methods for establishing the hazard maps and population exposure are approximate and simplified meant to cover large geographical areas. They are not intended for detailed local hazard mapping, but rather to obtain regional and national exposure data for comparison with other hazards. It should be noted that inundation maps are based on coarse topographic data (SRTM) hampered with inaccuracies and falsely elevated land. This may lead to an underestimation of the inundation and therefore also the exposure. The effect is particularly pronounced in tropical areas (Römer et al., 2012), but may also play an important role in urban areas. Moreover, the effects of countermeasures such as breakwaters which are expected to decrease the exposure are not considered. Breakwaters are for instance common in Japan. In the hazard maps, differences in the reference height of the coastline sections are sometimes encountered. These differences may cause slight offsets between the affected zones and coastlines.

4.4 Risk assessment

The tsunami risk may be defined as the product of the hazard, exposure, and vulnerability. The present study contains an analysis of the first two parts, while the vulnerability has not been addressed directly. To provide explicit comparison with other hazards, the tsunami risk needs to be quantified. Vulnerability and risk has not been quantified so far mainly for three reasons: A need to first prioritise tsunami hazard assessment and exposure as these are the primary input to a possible subsequent risk analysis; tsunami vulnerability has been sparsely studied prior to the Indian Ocean tsunami in 2004; vulnerability exhibits large local differences as demonstrated by the devastating tsunamis in 2004 and 2011; and reliable vulnerability models for present use do not exist. For instance, the lethality in Banda Aceh in 2004 was much higher than in Japan 2011 although the run-up heights were comparable. However, the economic loss was in turn much higher in Japan 2011 (<http://www.emdat.be>). How to interpret measures of vulnerability in future updates of GAR is not yet clear, but a future tsunami risk assessment should still be aimed at.

5 References

- Annaka, T., Satake, K., Sakakiyama, T., Yanagisawa, K., and Shuto, N. 2007. Logic-tree approach for probabilistic tsunami hazard analysis and its applications to the Japanese coasts. *Pure Appl. Geophys.* 164, 577-92.
- Berryman et al., (2005): Review of Tsunami Hazard and Risk in New Zealand. Institute of Geological & Nuclear Sciences client report 2005/104
- Bird, P. (2003). An updated digital model of plate boundaries. *Geochem. Geophys. Geosyst.*, 4(3): 1027, doi:10.1029/2001GC000252.
- Blaser, L., F. Krüger, M. Ohrnberger, and F. Scherbaum (2010), Scaling Relations of Earthquake Source Parameter Estimates with Special Focus on Subduction Environment, *Bull. Seis. Soc. Am.*, 100, 2914-2926
- Burbidge, D., Cummins, P.R., Mleczko, R., and Thio H.K. (2008), A Probabilistic Tsunami Hazard Assessment for Western Australia, *Pure and Applied Geophysics*, DOI 10.1007/s00024-008-0421-x, 2008.
- Carrier, G.F. and Greenspan, H.P. (1958), Water waves of finite amplitude on a sloping beach, *J. Fluid Mech.*, 4 97-109
- Cornell, C. A. (1968), Engineering seismic risk analysis, *Bull. Seismol. Soc. Am.*, 58, 1583–1606.
- GAR, (2009), Global Assessment Report 2009, URL: <http://www.preventionweb.net/english/hyogo/gar/2009/?pid:34&pif:3>
- Geist, E. and T. Parsons (2006): Probabilistic analysis of tsunami hazards. *Nat. Hazards*, 37, pp. 277-314.
- GMT (2011), The Generic Mapping Tool, URL: <http://gmt.soest.hawaii.edu/>
- González, F.I., E.L. Geist, B. Jaffe, U. Kânoğlu, H. Mofjeld, C.E. Synolakis, V.V. Titov, D. Arcas, D. Bellomo, D. Carlton, T. Horning, J. Johnson, J. Newman, T. Parsons, R. Peters, C. Peterson, G. Priest, A. Venturato, J. Weber, F. Wong, and A. Yalciner (2009), Probabilistic tsunami hazard assessment at Seaside, Oregon, for near- and far-field seismic sources. *J. Geophys. Res.*, 114, C11023, doi: 10.1029/2008JC005132
- Grilli S.T., Harris, J.C., Tajali Bakhsh, T.S., Tappin, D.R., Masterlark, T., Kirby, J.T., Shi, F., Ma, G., (2012), Recent progress in the nonlinear and dispersive modelling of tsunami generation and coastal impact: Application to Tohoku 2011, 13^{èmes} Journées de l'Hydrodynamique, 21-23 November 2012, Chatou, France
- Harbitz, C.B., S. Glimsdal, S. Bazin, N. Zamora, F. Løvholt, H. Bungum, H. Smebye, P. Gauer, O. Kjekstad (2012), Tsunami hazard in the Caribbean: Regional exposure derived from credible worst case scenarios. *Continental Shelf Research* 8, 1-23, doi:10.1016/j.csr.2012.02.006.

- Harbitz, C.B., F. Løvholt, and H. Bungum (2013): Submarine landslide tsunamis – how extreme and how likely? *Nat. Hazards, in press*
- Horspool, N., Pranantyo, I., Griffin, J., Latief, H., Natawidjaja, D.H., Kongko, W., Cipta, A., Bustaman, Anugrah, S.D., and Thio H.K. (in prep) A Probabilistic Tsunami Hazard Assessment for Indonesia. *Submitted to Nat. Hazards Earth Syst. Sci.*
- Kaistrenko, V.M., Pinegina, T., and Klyachko, M.A. (2003): Evaluation of tsunami hazard for the southern Kamchatka coast using historical and paleotsunami data. In Yalciner, Pelinovsky, Okal, and Synolakis (eds), *Submarine Landslides and Tsunamis*, 217-228, Kluwer Academic Publishers
- Kajiura, K. (1963), The leading wave of a tsunami, *Bull. Res. Inst.*, 41, 535–571.
- LandScan, (2007). High Resolution Global Population Data Set © UT-Battelle, LLC, Operator of Oak Ridge National Laboratory, USA.
- Løvholt, F., G. Pedersen, and S. Glimsdal, S., (2010), Coupling of dispersive tsunami propagation and shallow water coastal response, In Zahibo, N., Pelinovsky, E., Yalciner, A., and Titov, V. (eds.), *Proceedings of the “Caribbean Waves 2008” workshop in Guadeloupe Dec. 2008. The Open Oceanography Journal special volume.*
- Løvholt, F., Glimsdal, S., Harbitz, C.B., Zamora, N., Nadim, F., Peduzzi, P., Dao, H., Smebye, H. (2012a) Tsunami hazard and exposure on the global scale, *Earth-Sci. Rev.*, 110, 1–4, 58-73, ISSN 0012-8252, 10.1016/j.earscirev.2011.10.002.
- Løvholt, F., Kühn, D., Bungum, H., Harbitz, C.B., and Glimsdal, S. (2012b), Historical tsunamis and present tsunami hazard in eastern Indonesia and the southern Philippines, *J. Geophys. Res.*, 117, B09310, doi:10.1029/2012JB009425
- Løvholt, F., Lynett, P., and Pedersen, G. (2013), Simulating run-up on steep slopes with operational Boussinesq models; capabilities, spurious effects and instabilities. *Nonlin. Pro. Geophys., in press*
- Matias, L. M., Cunha, T., Annunziato, A., Baptista, M. A., and Carrilho, F.: Tsunamigenic earthquakes in the Gulf of Cadiz: fault model and recurrence, *Nat. Hazards Earth Syst. Sci.*, 13, 1-13, doi:10.5194/nhess-13-1-2013, 2013
- Nadim, F. and Glade, T.: On tsunami risk assessment for the west coast of Thailand, F. Nadim, R. Pöttler, H. Einstein, H. Klapperich, and Ste Kramer (Eds), ECI Symposium Series, 7. <http://services.bepress.com/eci/geohazards/28>, 2006.
- Okada, Y. (1985): Surface deformation due to shear and tensile faults in a half-space. *Bull. Seismic Soc. of Am.* 74, 4, pp. 1135-1154.
- Synolakis, C.E. Bernard, E.N., Titov, V.V., Kânoglu, U., and González, F. (2007), Validation and Verification of Tsunami Numerical Models, *Pure Appl. Geophys.* 165, 2197–2228

- Parsons, T., and Geist, E., 2009. Tsunami probability in the Caribbean Region. *Pure and App.Geoph.* 165: 2089-2116
- Pedersen, G., (2008). Modeling run-up with depth integrated equation models. *In Advanced Numerical Models for Simulating Tsunami Waves and Run-up*, Liu, P.L.-F., Yeh, H., and Synolakis, C. 3-41. World Scientific
- Pedersen, G. and Løvholt, F. (2008), Documentation of a global Boussinesq solver, *Preprint Series in Applied Mathematics 1*, Dept. of Mathematics, University of Oslo, Norway
- Pedersen, G. (2011), Oblique runup of non-breaking solitary waves on an inclined plane, *J. Fluid Mech.*, 668, 582–606, doi:10.1017/S0022112010005343
- Römer, H., Willroth, P., Kaiser, G., Vafeidis, A.T., Ludwig, R., Sterr, H. and Revilla Diez, J. (2012), Potential of remote sensing techniques for tsunami hazard and vulnerability analysis – a case study from Phang-Nga province, Thailand, *Nat. Hazards Earth Syst. Sci.*, 12, 2103-2126
- Satake, K., (1995) Linear and non-linear computations of the 1992 Nicaragua earthquake tsunامي. *Pure and Applied Geophysics*, 144, 455-470.
- Stein, S., and Okal, E.A, (2007), Ultralong Period Seismic Study of the December 2004 Indian Ocean Earthquake and Implications for Regional Tectonics and the Subduction Process, *Bull. Seism. Soc. Am.*, 97, S279–S295, doi:10.1785/0120050617
- Tiberti, M.M., Lorito, S., Basili R., Kastelic, V., Piatanesi, A., and Valensise, G. (2008), Scenarios of Earthquake-Generated Tsunamis for the Italian Coast of the Adriatic Sea, *Pure Appl. Geophys.* 165, 2117–2142
- Tinti S., Armigliato A., Zaniboni F., Pagnoni G. (2012), Influence of the heterogeneity of the seismic source on the timely detectability of a tsunami: implications for tsunami early warning in the central Mediterranean. *Proceedings of the 22nd International and Polar Engineering Conference, ISOPE-2012*, Rhodes, June 17-22, 2012.
- Thio H.K., Somerville P., and Polet J., (2010), Probabilistic Tsunami Hazard in California, *PEER Report 2010/108* Pacific Earthquake Engineering Research Center

Kontroll- og referanseside/ Review and reference page



Dokumentinformasjon/Document information					
Dokumenttittel/Document title UNISDR Global Assessment Report 2013 - GAR13 Tsunami methodology and results overview			Dokument nr./Document No. 20120052-02-R		
Dokumenttype/Type of document		Distribusjon/Distribution		Dato/Date 21 March 2012	
<input checked="" type="checkbox"/> Rapport/Report		<input checked="" type="checkbox"/> Fri/Unlimited		Rev.nr./Rev.No. 1	
<input type="checkbox"/> Teknisk notat/Technical Note		<input type="checkbox"/> Begrenset/Limited			
		<input type="checkbox"/> Ingen/None			
Oppdragsgiver/Client The United Nations Office for Disaster Risk Reduction – UNISDR					
Emneord/Keywords Tsunami, hazard assessment, population exposure, critical facilities					
Stedfesting/Geographical information					
Land, fylke/Country, County			Havområde/Offshore area		
Kommune/Municipality			Felt navn/Field name		
Sted/Location			Sted/Location		
Kartblad/Map			Felt, blokknr./Field, Block No.		
UTM-koordinater/UTM-coordinates					
Dokumentkontroll/Document control					
Kvalitetssikring i henhold til/Quality assurance according to NS-EN ISO9001					
Rev./Rev.	Revisjonsgrunnlag/Reason for revision	Egenkontroll/ Self review av/by:	Sidemannskontroll/ Colleague review av/by:	Uavhengig kontroll/ Independent review av/by:	Tverrfaglig kontroll/ Inter-disciplinary review av/by:
0	Original document	FLO	CH		CH
1	Revision based external peer review	Flo	CH		CH
Dokument godkjent for utsendelse/ Document approved for release		Dato/Date 2013.03.21		Sign. Prosjektleder/Project Manager Farrokh Nadim	

NGI er et internasjonalt ledende senter for forskning og rådgivning innen geofagene. Vi utvikler optimale løsninger for samfunnet, og tilbyr ekspertise om jord, berg og snø og deres påvirkning på miljøet, konstruksjoner og anlegg.

NGI arbeider i følgende markeder: olje og gass, bygg og anlegg, samferdsel, naturskade og miljøteknologi.

NGI er en privat stiftelse med kontor og laboratorier i Oslo, avdelingskontor i Trondheim og datterselskap i Houston, Texas, USA.

NGI ble utnevnt til "Senter for fremragende forskning" (SFF) i 2002, og leder "International Centre for Geohazards" (ICG).

www.ngi.no

NGI is a leading international centre for research and consulting in the geosciences.

NGI develops optimum solutions for society, and offers expertise on the behaviour of soil, rock and snow and their interaction with the environment, installations and structures.

NGI works within the oil and gas, building and construction, transportation, natural hazards and environment sectors.

NGI is a private foundation with office and laboratory in Oslo, branch office in Trondheim and daughter company in Houston, Texas, USA. NGI was awarded Centre of Excellence status in 2002, and leads the International Centre for Geohazards (ICG).

www.ngi.no



Hovedkontor/Main office:
PO Box 3930 Ullevål Stadion
NO-0806 Oslo
Norway

Besøksadresse/Street address:
Sognsveien 72, NO-0855 Oslo

Avd Trondheim/Trondheim office:
PO Box 1230 Pirsenteret
NO-7462 Trondheim
Norway

Besøksadresse/Street address:
Pirsenteret, Havnegata 9, NO-7010 Trondheim

T: (+47) 22 02 30 00
F: (+47) 22 23 04 48

ngi@ngi.no
www.ngi.no

Kontonr 5096 05 01281 /IBAN NO26 5096 0501 281
Org. nr./Company No.: 958 254 318 MVA

BSI EN ISO 9001
Sertifisert av/Certified by BSI, Reg. No. FS 32989

